

A NOVEL APPROACH FOR POLYGONAL ROOFTOP DETECTION IN SATELLITE/AERIAL IMAGERIES

Masoud S. Nosrati and Parvaneh Saeedi

School of Engineering Science, Simon Fraser University, Burnaby, BC, Canada
{smn6, psaeedi}@sfu.ca

ABSTRACT

This paper presents a new solution for automatic polygonal rooftop extraction (with no angular constraint) in satellite/aerial imageries based on line intersections. The proposed approach uses edge definitions and their relationships with each other to create a set of potential vertices. Using a graph representation, the relationship between potential vertices are studied in an efficient way. Polygonal rooftops correspond to closed loops in this graph. The experimental results for images acquired from Google Earth show that this solution has a high precision in detecting polygonal rooftops.

Index Terms— Building extraction, 3D map generation, polygonal building models, satellite imagery

1. INTRODUCTION

Extraction of buildings' 3D geometrical information from satellite images has become a key element in many geospatial applications such as urban city design and planning, military simulation, and site monitoring of a particular geographic location. Nowadays almost all operational systems for 3D building model reconstruction are semi-automated ones, where a skilled operator is involved in the 3D geometry modeling of building instances. In recent years, a number of automatic approaches have been proposed for quadrilateral building detection using edge/line detection techniques to extract buildings footprints.

Wei et al. [1] proposed a probabilistic modeling for buildings in dense urban areas in high-resolution images. With the assumption of a logistic function for building distribution function, they show a good recognition rate at a high computational cost. Li et al. [2] combined different techniques including image segmentation, region growing, and morphological methods. Their approach however could not detect buildings with the dark rooftops. Florent Lafarge et al. [3] used an object-based approach for automatic building extraction from DEMs. Peng and Liu [4] used Chengs image primitives with the modified partial snake model to detect buildings. Sohn and Dowman [5] suggested an automatic building

extraction technique using local Fourier analysis to determine the dominant orientation angle of a building cluster in dense urban areas. Wei et al. [6] proposed an unsupervised clustering algorithm to separate shadows from other parts of a scene. The shadow and its directions were used to verify the presence of a building structure. They utilized Canny edge detector and Hough transform to refine buildings' boundaries. Liu et al. [7] proposed an approach based on multi-scale object oriented classification and probabilistic Hough transform to detect rectangular buildings roofs. Jin and Davis [8] introduced an automatic system that utilized structural, contextual and spectral information to detect buildings in satellite imagery. They reported an extraction rate of 72.7% with 58.8% quality.

This paper presents a new methodology for automatic polygonal shape rooftop extraction with no angular constraint in remotely sensed images. The suggested approach is based on examining lines and their existing or potential intersections using a graph presentation. Finding a polygonal shape in the image corresponds to finding a loop in the graph. The tree structure and backtracking algorithm are implemented for an efficient search for potential building hypotheses. Local refinements are also employed to verify the quality of identified hypotheses and to reject outliers. The performance of the system is assessed using detection rate and McKeown's shape accuracy factor [9].

2. METHODOLOGY

2.1. Pre-processing and corner detection

The goal of this part is to find the most distinctive edge and corner features in the image. Some pre-processing including a morphological opening followed by a closing are applied to smooth all small objects including chimneys on the rooftops or ruling on the streets. Canny edge detector is then applied on the resultant image followed by an edge linking process. All short edges after this process are removed from the remaining process. A line fitting algorithm with a maximum deviation of 2 pixels is then applied on the detected edges. In the next step all *possible corners* are extracted from the gray scale image. The term *possible corner* includes both inter-

This work was supported by the Canadian Natural Sciences and Engineering Research Council's Strategic Grant Program.

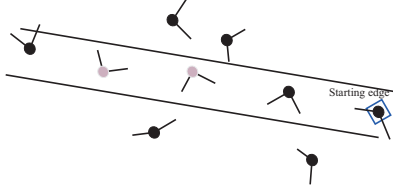


Fig. 1. Searching corners along one side of the starting corner.

sections of lines that in fact intersect within the image and those potential intersections that their parent line segments do not intersect in the image but their continuation will. Each detected corner is associated with the angle between the two parent lines. These corners are used in creating a graph in which each corner represents a vertex and two edges. Detecting polygonal rooftop hypotheses corresponds to the problem of detecting closed loops in this graph.

2.2. Searching for loops in the graph

In order to detect loops in the corner graph, a dynamic programming approach is employed. Here each loop is defined with a set of vertices and edges. Starting from every corner, a path along one of the corner's edges is selected. A tube shape window with a width of w pixels and a length of d_{max} pixels is placed on the image. d_{max} is a configurable parameter that represents the maximum length of a building hypothesis. In this window, a search is performed for all corners with one edge in the same direction as the starting edge.

Figure 1 displays two found candidate corners (shown with light colors) each with one side approximately (a difference of $\pi/4$ degrees is tolerated) in the opposite direction as the starting edge. After finding all candidate corners in the current searching level, a filtering process is performed to remove outlier corners. Following conditions are used for outliers' rejection:

1. Minimum distance between corners at level n and level $n + 1$ must be greater than d_{min} . d_{min} is the minimum length for a building's side.
2. Maximum distance between the corners at level n and a corner at level $n + 1$ must be less than d_{max} .
3. There must exist a physical edge between the corners at levels n and $n + 1$. The length of the edge(s) between the two levels corners must be greater than $w_l \times d_{cl}$. w_l is a weight coefficient, $w_l \in [0 1]$, and d_{cl} is the Euclidean distance between the two levels' corners.

At this point, each candidate corner's edge is indexed as either *in* or *out*. The edge on the opposite direction is indexed as *in* and the other as *out*, Figures 2. In order to find the loop, for every candidate corner at level n , all candidate corners at

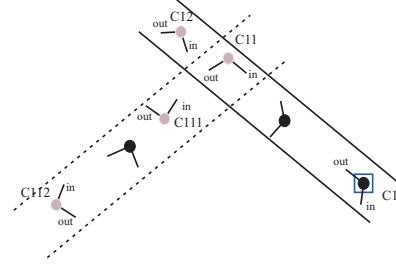


Fig. 2. Directional search for corners.

level $n + 1$ will be found and filtered. A maximum value of 8 (N_{max}) is utilized for the level parameter in this work. This implies that the search for polygons with a maximum 8 sides will carry out.

In the tree structure, the forward tracking starts at level 0 with the first corner, C_1 . It traverses down to find all candidate corners until C_1 is met again. If, however, the N_{max} is reached before reaching to C_1 again, the backward tracking will start. In each backward tracking attempt, only one level lower is inspected. If at that level there is another candidate corner left, the forward tracking once again is initiated and otherwise the backward tracking will move on to one level lower. If the lowest level (0) is reached, a new corner is chosen and the process will continue. At the end of this process, after all corners at level 0 are inspected, all potential rooftop candidates are detected. Here the use of tree structure with a back tracking scheme achieves faster rooftop identification.

2.3. Hypothesis refinement

Generally, for each true building several candidate rooftop hypotheses are detected that vary only slightly. In this section a two-step filtering scheme is implemented that removes weak hypotheses.

1. In the first step, the standard deviation of pixels' gray level values within each hypothesis is calculated. Only hypotheses with small standard deviation are kept.
2. In the second step, image intensities inside and outside each hypothesis are inspected. The relative gray level difference between the rooftop surface points and outside points is calculated. If this difference is small the candidate hypothesis will be filtered out.

2.4. Hypothesis retrieval

Occasionally, true hypothesis corresponding to actual buildings would be removed due to parameters setting sensitivity. To recover such hypotheses after first step in Section 2.3, hypotheses that are physically close to each other are grouped into one group. The number of created groups defines the



Fig. 3. Detected rooftops for scene 3.

potential number of rooftop hypotheses that could exist in the image. Now, if after above refinements, the number of detected hypotheses is smaller than the number of identified groups, a recursive local retrieving process will be initiated. To ensure that the true hypotheses are not removed, due to the setting values of the global parameters, the sensitivity of some parameters will be automatically adjusted. These parameters include the number of corners, rooftop intensity variation threshold, and the threshold associated with intensity variation on inside and outside of the hypothesis definition. Each iteration follows with a refinement process. If after 5 successive iterations, no hypothesis is obtained, the missing group will be eliminated and otherwise a new rooftop hypothesis will be added to the detected hypotheses.

2.5. Hypothesis merging

Connected buildings with apparent edge on their roof top could be identified as one or two buildings. In this system, if the apparent edge is strong, two hypotheses will be detected. Therefore a search among all extracted hypotheses will be initiated. Hypotheses with a distance smaller than a predefined threshold are combined together into one.

3. EXPERIMENTAL RESULTS

The proposed system was tested on 18 different satellite test images that were acquired from Google Earth. Figures 3 to 6 represents some detection examples.

To evaluate the algorithms quantitatively, three metrics are employed: Detection Rate (DR), False Negative Rate (FNR), and the McKeown's shape accuracy factor [9].

$$\begin{cases} DR = \frac{N_{TP}}{N_{TP} + N_{FP}} \\ FNR = \frac{N_{FN}}{N_{FN} + N_{TP}} \end{cases} \quad (1)$$

Here, TP , FP and FN represent True Positives, False Positives and False Negatives in each scene. To calculate the McKeown's factor the areas of buildings in the ground truth is compared against the areas of the detected buildings.

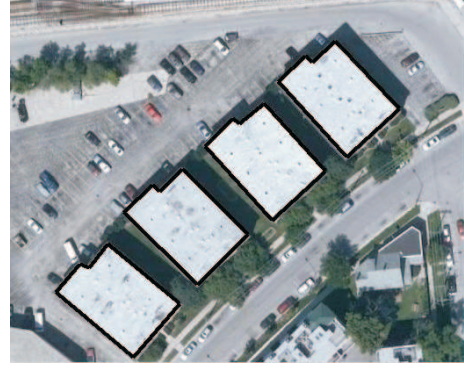


Fig. 4. Detected rooftops for scene 4.



Fig. 5. Detected rooftops for scene 15.

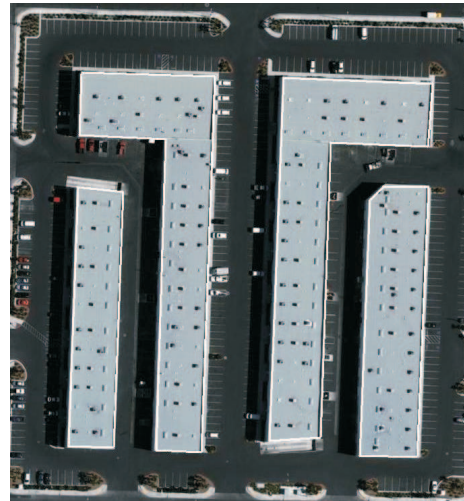


Fig. 6. Detected rooftops for scene 16.

Table 1. Summary of the detection results.

Scene No.	Total No. of Buildings	No. of TP	d_{min}	No. of FP	No. of FN	DR %	FNR %
1	4	4	42	0	0	100	0
2	2	2	40	0	0	100	0
3	3	3	65	0	0	100	0
4	4	4	8	0	0	100	0
5	2	2	35	0	0	100	0
6	3	2	70	1	1	66	33
7	38	35	20	3	3	92	7.8
8	10	10	14	1	0	90	0
9	2	2	23	1	0	66	0
10	4	4	75	0	0	100	0
11	13	13	18	0	0	100	0
12	3	3	12	0	0	100	0
13	4	4	30	0	0	100	0
14	19	18	11	0	1	100	5
15	9	9	35	0	0	100	0
16	4	4	20	0	0	100	0
17	3	3	25	0	0	100	0
18	5	5	80	0	0	100	0

Table 2. Comparison of the average DR.

Method	Average DR
Wei et al. [6]	68.9%
Jin et al. [8]	72.7%
Wei et al. [1]	84.3%
Proposed method	95.2%

$$\text{Shape accuracy} = 1 - \frac{|A_{GT} - A_{BD}|}{A_{GT}} \times 100 \quad (2)$$

A_{GT} and A_{DB} represent areas of a building in the ground truth and the detected hypothesis by the proposed system. The mean shape accuracy of the proposed method is 96.5% which is substantially more than the value reported in [8], 58.8%. Table 1 summarizes results for all test images. In computing these results, partial buildings on the image (near to the image sides) are not included. Also buildings with at least one dimension equal or smaller than d_{min} are excluded from the results presented in this table. Here, parameter d_{min} is twiggled between different runs of the program for different images. The reason for this is merely the running time complexity. Table 2 compares the performance of some of the previous work with that of the proposed method.

4. CONCLUSIONS

This paper introduced a new method for detecting buildings with polygonal footprints in satellite/aerial images. In this approach all corners are detected by intersecting lines. The orientation of the parent lines was incorporated as a feature for each corner. These corners are utilized to create a graph. Detecting buildings in an image corresponds to finding loops in this graph. A back tracking algorithm was incorporated to search the graph in a fast manner. Experimental results show the performance superiority of the proposed method.

5. REFERENCES

- [1] L. Wei and V. Prinet, "Building detection from high-resolution satellite image using probability model," *IGARSS*, vol. 6, pp. 3888–3891, July 2005.
- [2] H.Y. Li, H.Q. Wang, and C.B. Ding, "A new solution of automatic building extraction in remote sensing images," *IGARSS*, pp. 3790–3793, July 2006.
- [3] F. Lafarge, X. Descombes, J.B. Zerubia, and M. Pierrot Deseilligny, "Automatic building extraction from dems using an object approach and application to the 3d-city modeling," *PandRS*, vol. 63, no. 3, pp. 365–381, May 2008.
- [4] J. Peng and Y. C. Liu, "Model and context-driven building extraction in dense urban aerial images," *IJRS*, vol. 26, pp. 1289–1307(19), April 2005.
- [5] G. Sohn and I. J. Dowman, "Extraction of buildings from high resolution satellite data," in *Automated Extraction of Man-Made Objects from Aerial and Space Images (III)*. Balkema Publishers, 2001, pp. 339–348.
- [6] Y. Wei, Z. Zhao, and J. Song, "Urban building extraction from high-resolution satellite panchromatic image using clustering and edge detection," *IGARSS*, pp. 2008–2010, 2004.
- [7] J. and Liu W.P. Liu, Z.J. and Wang, "Automated building extraction from high-resolution satellite imagery in urban areas using structural, contextual, and spectral information," *IGARSS*, vol. 4, pp. 2250–2253, 2005.
- [8] X. Jin and C.H. Davis, "Automated building extraction from high-resolution satellite imagery in urban areas using structural, contextual, and spectral information," *EURASIP Journal on Applied Signal Processing*, vol. 2006, no. 1, pp. 2196–2206, 2005.
- [9] D.M. McKeown, T.M. Bulwinkle, S. Cochran, W. Harvey, C. McGlone, and J.A. Shufelt, "Performance evaluation for automatic feature extraction," *International Archives of Photogrammetry and Remote Sensing 33 (Part B2)*, p. 379394, 2000.